Correlation trends in the hyperfine structures of ^{210,212}Fr

B. K. Sahoo,[1,*] D. K. Nandy,[1] B. P. Das,[2] and Y. Sakemi[3]

[1]*Theoretical Physics Division, Physical Research Laboratory, Navrangpura, Ahmedabad 380009, India*

[2]*Theoretical Physics and Astrophysics Group, Indian Institute of Astrophysics, Bangalore 560034, India*

[3]*Cyclotron and Radioisotope Center, Tohoku University, Sendai, Miyagi 980-8578, Japan*

(Received 19 January 2015; published 21 April 2015)

We demonstrate the importance of electron correlation effects in the hyperfine structure constants of many low-lying states in ^{210}Fr and ^{212}Fr. This is achieved by calculating the magnetic dipole and electric quadrupole hyperfine structure constants using the Dirac-Fock approximation, second-order many-body perturbation theory, and the coupled-cluster method in the singles and doubles approximation in the relativistic framework. By combining our recommended theoretical results with the corresponding experimental values, improved nuclear magnetic dipole and electric quadrupole moments of the above isotopes are determined. In the present work, it is observed that there are large discrepancies between the hyperfine structure constants of the $7D_{5/2}$ state obtained from the experimental and theoretical studies, whereas good agreement is found for the other $D_{5/2}$ states. Our estimated hyperfine constants for the $8P$, $6D$, $10S$, and $11S$ states could be very useful as benchmarks for the measurement of these quantities.

DOI: 10.1103/PhysRevA.91.042507 PACS number(s): 31.30.Gs, 21.10.Ky, 31.15.−p, 32.10.Fn

I. INTRODUCTION

Francium (Fr) is the heaviest alkali-metal atom in the periodic table, possessing 87 electrons. Therefore, the properties of this system are expected to exhibit moderately strong correlation effects, and their determination calls for using powerful many-body methods. The Fr atom, because of its large atomic number Z, is being considered for many important experimental studies. A few prominent examples among them are the measurements of the electric dipole moment (EDM) due to parity and time-reversal symmetries [1,2] and parity nonconservation (PNC) effects due to neutral weak interaction [2,3] and the nuclear anapole moment [4]. Like the EDM and PNC interactions, the magnetic dipole hyperfine interaction has a fairly strong dependence on Z [5] as it involves electrons interacting with the nucleus. Thus, theoretical investigations of hyperfine structures are necessary for EDM and PNC studies to test the accuracies of the wave functions in the nuclear region [6,7]. On the other hand, comparison of theoretical results from various approximations with the experimental values can provide a comprehensive understanding of the passage of electron correlations from lower to higher levels of many-body theory. This knowledge is essential to validate the theoretical results when experimental data are unavailable. Attempts have been made to investigate trends in the correlation effects in the calculations of hyperfine structure constants of the $S-$ states using lower-order many-body methods [8–11], but such trends have not been demonstrated explicitly for states of Fr having higher angular momenta.

The focus of this paper is the study of variation in the trends of correlation effects in the evaluation of the hyperfine structure constants of as many as 17 low-lying states in Fr using the relativistic second-order many-body perturbation theory [MBPT(2) method] and the coupled-cluster (CC) method at various levels of approximation using the reference state obtained by the Dirac-Fock (DF) method with V^{N-1} potential. In the present work, we have undertaken theoretical studies of the hyperfine structure constants of ^{210}Fr and ^{212}Fr isotopes for two reasons. First, ^{210}Fr has been proposed as one of the most suitable Fr isotopes for both the PNC and EDM studies [1,2]. To draw meaningful conclusions and to be consistent in the findings from comparisons between the theoretical and experimental hyperfine structure constants of different states, it is necessary to consider the results for as many states as possible for both the isotopes. The second, but essential, reason behind considering the above two isotopes is that experimental results of the hyperfine structure constants for only a few selective low-lying states of ^{210}Fr [12–15] and some other excited states of ^{212}Fr are available [16].

II. THEORY

The Hamiltonian describing the noncentral form of the hyperfine interaction between the electrons and nucleus in an atomic system is expressed in terms of the tensor operator products as [17]

$$H_{\rm hf} = \sum_k \mathbf{M}_n^{(k)} \cdot \mathbf{O}_{hf}^{(k)}, \tag{1}$$

where $\mathbf{M}_n^{(k)}$ and $\mathbf{O}_{\rm hf}^{(k)}$ are the spherical tensor operators with rank k (> 0) in the nuclear and electronic coordinates, respectively. These interaction strengths become weaker with higher values of k, so we consider only up to $k = 2$ in the present case. Due to the coupling between the electronic (J) and nuclear (I) angular momenta, the hyperfine states $|\gamma I J; F M_F\rangle$ are the proper bases with total angular momentum $\mathbf{F} = \mathbf{J} + \mathbf{I}$ and corresponding azimuthal quantum number M_F and γ representing the rest of the unspecified quantum numbers.

The energy splitting due to the first-order correction in the atomic state $|JM\rangle$ because of the hyperfine interactions is

*bijaya@prl.res.in

given by

$$W^{(1)}_{F,J} = \langle \gamma IJ; FM_F| \sum_k \mathbf{M}^{(k)}_n . \mathbf{O}^{(k)}_{\rm hf} |\gamma IJ; FM_F\rangle$$
$$= \sum_k (-1)^{I+J+F} \begin{Bmatrix} J & I & F \\ I & J & k \end{Bmatrix} \times \langle I|\big|M^{(k)}_n\big||I\rangle\langle J|\big|O^{(k)}_{\rm hf}\big||J\rangle, \quad (2)$$

which after expanding up to multipoles $k = 2$, gives

$$W^{(1)}_{F,J} = W^{M1}_{F,J} + W^{E2}_{F,J}, \quad (3)$$

where $W^{M1}_{F,J}$ and $W^{E2}_{F,J}$ are the contributions due to the magnetic dipole ($M1$) with $k = 1$ and electric quadrupole ($E2$) with $k = 2$ interactions, respectively. It is commonly expressed as

$$W^{M1}_{F,J} = \tfrac{1}{2} A_{\rm hf} K \quad (4)$$

and

$$W^{E2}_{F,J} = B_{\rm hf} \frac{\frac{3}{4}K^2 + \frac{3}{4}K - I(I+1)J(J+1)}{2I(2I-1)J(2J-1)} \quad (5)$$

with the hyperfine structure constants defined as

$$A_{\rm hf} = \mu_N g_I \frac{\langle J|\big|O^{(1)}_{\rm hf}\big||J\rangle}{\sqrt{J(J+1)(2J+1)}} \quad (6)$$

and

$$B_{\rm hf} = 2Q \left[\frac{2J(2J-1)}{(2J+1)(2J+2)(2J+3)}\right]^{1/2} \langle J|\big|O^{(2)}_{\rm hf}\big||J\rangle, \quad (7)$$

where μ_N is the nuclear Bohr magneton; $g_I = \frac{\mu_I}{I}$; μ_I and Q are the nuclear magnetic and quadrupole moments, respectively; and $K = F(F+1) - I(I+1) - J(J+1)$. It appears from the above expressions that the quantities $A_{\rm hf}/g_I$ and $B_{\rm hf}/Q$ are independent of nuclear factors, but these values can vary slightly among isotopes due to different nuclear potentials experienced by the electrons in these systems.

III. METHOD OF CALCULATIONS

The wave function ($|\Psi_n\rangle$) of an atomic state corresponding to the closed-shell configuration [$6p^6$] and a valence orbital n in Fr can be expressed as [18]

$$|\Psi_n\rangle = \Omega_n |\Phi_n\rangle, \quad (8)$$

where Ω_n is known as the wave operator, and it generates virtual excitations from the reference state $|\Phi_n\rangle$ to create all the possible excited configurations that are necessary to construct the atomic states $|\Psi_n\rangle$. The choice of $|\Phi_n\rangle$ is crucial for obtaining accurate results; we construct these determinantal states with orbitals generated using the V^{N-1} potential. These states can be expressed as $|\Phi_n\rangle = a^\dagger_n|\Phi_0\rangle$, where the DF wave function $|\Phi_0\rangle$ of the closed-core [$6p^6$] is obtained by considering the Dirac-Coulomb (DC) Hamiltonian ($H_{\rm DC}$) and is treated as the reference state for all the atomic states that we have considered.

The electron correlation effects are accounted for via Ω_n in the evaluation of $|\Psi_n\rangle$ in two steps. In the first step, we consider correlation effects within the closed-shell configuration [$6p^6$], following which we take into account correlation of the valence electron coupling with the core electrons to generate the virtual excitations. For this purpose, we express Ω_n as

$$\Omega_n = \Omega_0 + \Omega^v_n, \quad (9)$$

where Ω_0 (independent of n) has correlation effects from the closed-shell core while Ω^v_n contains correlation effects involving the electron from the valence orbital. In the perturbative expansion, we write [18]

$$\Omega_n = \sum_{k=0}^{2} \Omega^{(k)}_n \quad (10)$$

with $\Omega^{(k)}_n$ representing components of the wave operator carrying out k residual Coulomb interactions among the electrons. Using this formulation, hyperfine structure constants due to $O^{(1)}_{\rm hf}$ and $O^{(2)}_{\rm hf}$ (commonly denoted by O) are calculated as

$$\frac{\langle\Psi_n|O|\Psi_n\rangle}{\langle\Psi_n|\Psi_n\rangle} = \frac{\langle\Phi_n|\Omega^\dagger_n O \Omega_n|\Phi_n\rangle}{\langle\Phi_n|\Omega^\dagger_n\Omega_n|\Phi_n\rangle} = \frac{\langle\Phi_n|\sum_{i,j}\Omega^{(i)\dagger}_n O \Omega^{(j)}_n|\Phi_n\rangle}{\langle\Phi_n|\sum_{i,j}\Omega^{(i)\dagger}_n\Omega^{(j)}_n|\Phi_n\rangle}. \quad (11)$$

For the MBPT(2) method, $i + j \leqslant 2$ in the above summations.

In the Fock-space CC approach, we define $\Omega_0 = e^T$ and $\Omega^v_n = e^T S_n$, which for a single valence system yields the form

$$|\Psi_n\rangle = e^T\{1 + S_n\}|\Phi_n\rangle, \quad (12)$$

where T and S_n are the excitation operators involving core and core-valence electrons, respectively. Since our reference state is $|\Phi_0\rangle$, we take S_v in normal order with respect to $|\Phi_0\rangle$ for which, in the above expression, it is mentioned within curly braces. It is worthwhile to mention that T is also in normal order with respect to $|\Phi_0\rangle$ by construction. From a practical point of view we only consider the singles and doubles excitations through the CC operators, known as the CCSD method in the literature [19,20], by defining

$$T = T_1 + T_2 \quad \text{and} \quad S_n = S_{1n} + S_{2n}. \quad (13)$$

Even though we have used the CCSD approximation, we are able to include many important contributions from the triples and quadruples through the nonlinear terms of Eq. (12). In order to understand the role of these contributions in Fr for accurate evaluation of the hyperfine structure constants, we also determine contributions only from the linear terms of Eq. (12) by approximating

$$|\Psi_n\rangle = \{1 + T_1 + T_2 + S_{1n} + S_{2n}\}|\Phi_n\rangle, \quad (14)$$

which we refer to as the LCCSD method. This approximation resembles the singles and doubles configuration interaction (CISD) method.

The hyperfine structure constants are determined in the CC method as

$$\frac{\langle\Psi_n|O|\Psi_n\rangle}{\langle\Psi_n|\Psi_n\rangle} = \frac{\langle\Phi_n|\{1 + S^\dagger_n\}e^{T^\dagger} O e^T\{1 + S_n\}|\Phi_n\rangle}{\langle\Phi_n|\{1 + S^\dagger_n\}e^{T^\dagger}e^T\{1 + S_n\}|\Phi_n\rangle}. \quad (15)$$

The above expression has two nonterminating series $e^{T^\dagger} O e^T$ and $e^{T^\dagger}e^T$ in the numerator and denominator, respectively.

To account for the contributions that are significant from these series, we have used Wick's general theorem to divide these terms into effective one-body, two-body, and three-body terms [18]. The effective one-body terms are dominant owing to the single-particle form of the above O operators. They are computed self-consistently and stored as intermediate parts before contracting with the corresponding S_n operators. While the effective two-body and three-body terms are computed directly, we also reuse the effective one-body terms to construct the effective two-body and three-body terms. To illustrate the computational procedure adopted in our calculations, we outline the important steps below. First of all, we calculate the effective one-body terms of $e^{T^\dagger}e^T$ and store them as hole-hole (h-h), particle-particle (p-p), and particle-hole (p-h) blocks. The p-h block is first evaluated considering only linear terms and then stored as an intermediate effective p-h block which is then contracted further with an extra $T_2^\dagger$ operator to get the h-p block. Consequently, the p-h block is obtained from the h-p block by multiplying appropriate phase factors and the procedure is repeated until self-consistent results with tolerance 1×10^{-8} are achieved. Following this, the h-h and p-p blocks are constructed considering the direct contractions among the T_2 and $T_2^\dagger$ operators and along with the contractions of the h-p and h-p blocks with the T_1 operators. As a result, the h-h and p-p blocks still contain terms from infinite series through the h-p and p-h blocks. In a similar fashion we compute $e^{T^\dagger}Oe^T$ but by slightly modifying the above strategy. Here we make use of the effective one-body terms of $e^{T^\dagger}e^T$ for the construction of the effective one-body diagrams of $e^{T^\dagger}Oe^T$ and special attention has been paid to avoid the repetition of any diagram through the iterative procedure. We also replaced the T_1 and its conjugate operators appearing in the effective two-body and three-body terms of $e^{T^\dagger}Oe^T$ by the effective p-h and h-p blocks of $e^{T^\dagger}e^T$, respectively, to improve the results due to inclusion of the contributions from the higher-order CC terms.

We also estimate contributions from the important triple excitations considering them perturbatively in the above property evaluation expression by defining a triple excitation operator

$$S_{3n}^{\rm pert} = \frac{1}{4}\sum_{ab,pqr}\frac{(H_{\rm DC}T_2 + H_{\rm DC}S_{2n})_{abn}^{pqr}}{\epsilon_n+\epsilon_a+\epsilon_b-\epsilon_p-\epsilon_q-\epsilon_r}, \tag{16}$$

where a,b and p,q,r indices represent for the core and virtual orbitals, respectively. Particles appearing in the subscripts are annihilated while those appearing in the superscripts are created in the course of defining excitation processes. We refer to this approach as the CCSD$_{\rm t3}$ method in this work.

We use a recently developed basis function having the analytic exponential form with quadratic exponents to express the single-particle wave functions. These functions for the orbitals having orbital angular momentum value l are given as

$$|\phi^l(r)\rangle = r^l\sum_{\nu=1}^{N_l}c_\nu^l e^{-\alpha_\nu r^4}|\chi(\theta,\varphi)\rangle, \tag{17}$$

where $|\chi(\theta,\varphi)\rangle$ represents for the angular momentum part, N_l corresponds to the total number of analytic functions considered in the calculations, and α_ν is an arbitrary coefficient constructed satisfying the even tempering condition between two parameters α_0 and β as

$$\alpha_\nu = \alpha_0\beta^{\nu-1}. \tag{18}$$

The motive for using the above analytic function is to describe the atomic wave functions more accurately than the Slater- and Gaussian-type orbitals in the nuclear region of a heavy atom like Fr. We give the list of parameters in Table I that are used in the present calculations.

TABLE I. List of different parameters of bases used in the present calculations.

	s	p	d	f	g
N_l	40	39	38	37	36
α_0	2.0×10^{-8}	2.5×10^{-8}	2.5×10^{-8}	2.1×10^{-1}	2.1×10^{-7}
β	5.06	5.04	5.06	5.08	5.15

We consider a two-parameter Fermi-charge distribution to account for the finite size of the nucleus as

$$\rho_n(r) = \frac{\rho_0}{1+e^{(r-b)/a}}, \tag{19}$$

for the normalization factor ρ_0, the half-charge radius b, and $a = 2.3/4(\ln 3)$ is related to the skin thickness, while we evaluate the nuclear potential. We have used $a = 2.3/4(\ln 3)$, but $b = 6.7032$ fm and $b = 6.7166$ fm for ^{210}Fr and ^{212}Fr, respectively, that are determined using the relation

$$b = \sqrt{\frac{5}{3}r_{\rm rms}^2 - \frac{7}{3}a^2\pi^2}, \tag{20}$$

by taking the respective values for the root-mean square (rms) charge radii of the nuclei $r_{\rm rms}$ from the nuclear data table [21].

IV. RESULTS AND DISCUSSION

In order to demonstrate the propagation of electron correlation effects from the lower to higher orders of many-body methods, we present results using the DF, MBPT(2), LCCSD, CCSD, and CCSD$_{t3}$ methods for $A_{\rm hf}/g_I$ and $B_{\rm hf}/Q$ of the first 17 low-lying states of ^{210}Fr in Table II. We find changes beyond the third decimal places in these results for all the states except for the $A_{\rm hf}/g_I$ values of the S states, which are reduced by -1.141, -0.242, -0.095, -0.047, and -0.028 (in MHz) in the $7S$, $8S$, $9S$, $10S$, and $11S$ states, respectively, of ^{212}Fr compared to the results of ^{210}Fr. We account for these differences later while considering the results for ^{212}Fr. It can be seen from the above table that the MBPT(2) results are larger than the corresponding DF results for both the properties except for the $A_{\rm hf}/g_I$ values of the $D_{5/2}$ states. In fact, there are sign differences between the DF and MBPT(2) results of $A_{\rm hf}/g_I$ in the $D_{5/2}$ states, implying that correlation effects are very strong for these states. It is found that the LCCSD method yields much larger values for both $A_{\rm hf}/g_I$ and $B_{\rm hf}/Q$ compared to the other methods. The nonlinear terms in the CCSD methods contribute substantially but with opposite sign to reduce the LCCSD values. Triples through the CCSD$_{\rm t3}$ method also further reduce the $A_{\rm hf}/g_I$ values while they lead to small increases in the values of $B_{\rm hf}/Q$. Thus, we conclude

TABLE II. Results for $A_{\rm hf}/g_I$ and $B_{\rm hf}/Q$ obtained using the DF, MBPT(2), LCCSD, CCSD, and CCSD$_{\rm t3}$ methods. Previously reported calculations using varieties of many-body methods are also quoted as "Others".

	$A_{\rm hf}/g_I$ (MHz)						$B_{\rm hf}/Q$ (MHz)					
State	DF	MBPT(2)	LCCSD	CCSD	CCSD$_{\rm t3}$	Others	DF	MBPT(2)	LCCSD	CCSD	CCSD$_{\rm t3}$	Others
$7s\ ^2S_{1/2}$	6531.06	10186.68	11457.29	9916.20	9885.24	9927.69[a]						
						9947.07[b]						
						10155.40[c]						
						8432.65[d]						
$7p\ ^2P_{1/2}$	707.70	1169.41	1522.50	1281.84	1279.56	1308.67[b]						
						1265.77[c]						
						876.12[e]						
$7p\ ^2P_{3/2}$	55.68	97.20	124.80	104.34	104.28	103.38[b]	118.03	234.51	300.47	258.99	259.73	231[e]
						115.09[c]						
						96.28[e]						
$6d\ ^2D_{3/2}$	36.24	44.10	123.00	85.02	85.20		26.19	73.47	100.17	96.33	98.61	
$6d\ ^2D_{5/2}$	14.28	−23.04	−84.36	−58.92	−58.82		30.34	97.09	134.01	129.38	131.40	
$8s\ ^2S_{1/2}$	1674.12	2234.40	2337.92	2159.16	2151.90	2160.98[a]						
						2165.88[b]						
						2218.47[c]						
						2155.27[d]						
$8p\ ^2P_{1/2}$	251.76	381.06	457.38	402.84	402.01	408.68[b]						
						409.46[c]						
$8p\ ^2P_{3/2}$	20.40	33.96	40.62	35.04	35.03	34.25[b]	43.29	78.74	94.73	83.81	84.01	
						39.64[c]						
$7d\ ^2D_{3/2}$	18.30	16.14	36.45	30.84	30.90		13.23	24.99	29.28	29.97	30.53	
$7d\ ^2D_{5/2}$	6.90	−12.24	−18.62	−16.32	−16.28		14.57	32.84	38.56	39.45	39.92	
$9s\ ^2S_{1/2}$	687.54	881.28	910.01	852.78	849.72	852.39[a]						
						839.40[d]						
$10s\ ^2S_{1/2}$	382.38	468.12	449.63	455.82	454.26	402.97[d]						
$8d\ ^2D_{3/2}$	9.38	7.75	16.62	14.45	14.47		6.79	9.47	13.15	13.43	13.66	
$8d\ ^2D_{5/2}$	3.46	−5.34	−7.62	−6.90	−6.88		7.35	12.62	17.26	17.59	17.78	
$9d\ ^2D_{3/2}$	5.08	4.22	9.13	7.84	7.86		3.68	5.01	7.08	7.12	7.24	
$9d\ ^2D_{5/2}$	1.87	−3.02	−3.89	−3.53	−3.52		3.96	6.74	9.21	9.25	9.35	
$11s\ ^2S_{1/2}$	186.13	238.72	252.16	231.13	230.12	208.11[d]						

[a]Reference [15].
[b]Reference [22].
[c]Reference [23].
[d]Reference [11].
[e]Reference [24].

that the correlation effects represented by the nonlinear terms that correspond to the triple and quadruple excitations are crucial for the accurate evaluation of the hyperfine structure constants of the Fr atom.

We also mention about previously reported calculations of $A_{\rm hf}/g_I$ and $B_{\rm hf}/Q$ in Fr in Table II as "Others" [11,15,22–24]. Owusu *et al.* investigated the core-polarization effects systematically in the $S-$ states of ^{212}Fr using the relativistic many-body perturbation theory. These values are found to be smaller than our MBPT(2) results. The singles and doubles with partial triples all-order (SDpT) method, which is analogous to our LCCSD approximation but with important triples effects in the wave-function determination, was employed in Refs. [15,22] to evaluate the $A_{\rm hf}/g_I$ values of a few low-lying states and is in close agreement with our CCSD and CCSD$_{\rm t3}$ results. Dzuba *et al.* employed a restricted Hartree-Fock method in the relativistic framework and incorporated correlation effects using many-body perturbation theory to investigate correlation effects in the hyperfine structure constants of a few low-lying states of ^{211}Fr [23]. Heully and Mårtensson-Pendrill used a relativistic many-body perturbation method treating polarization effects to all orders [24]. Their results differ significantly from our calculations.

To understand the role of various correlation effects in the evaluation of the $A_{\rm hf}/g_I$ values for the states belonging to different angular momenta, we discuss here their trends by plotting individual contributions from a few important CCSD terms. This knowledge is of immense interest for the theoretical studies of PNC and EDM properties in a Fr atom [6,7]. As demonstrated explicitly by us earlier [25,26], the OS_{1v} and OS_{2v} terms from the CCSD method correspond to all-order pair-correlation and core-polarization effects, respectively. Similarly, correlation effects through the OT_1 CC term can be interpreted as the core-valence correlations that were missing in the generation of the single particle orbitals using the V^{N-1} DF potential. Therefore, the DF value

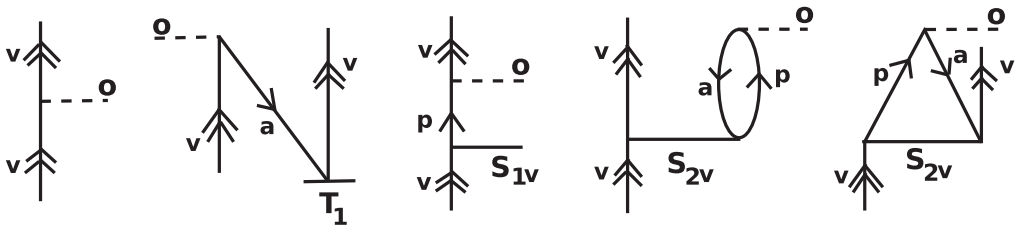

FIG. 1. Goldstone diagrammatic representation of O, OT_1, OS_{1v}, and OS_{2v} terms corresponding to the DF and correlation contributions to the hyperfine structure constants. Lines with double arrows or a single arrow pointing upwards denote valence (v) and virtual particle (p) orbitals, respectively, while lines with a downward arrow stand for the occupied orbitals (a).

with the correlation contributions from the OT_1, OS_{1v} (which also contains the DF value at its lowest order) and OS_{2v} CCSD terms make the dominant contributions in the evaluation of the properties that we have considered. Diagrammatic representations of these terms are shown in Fig. 1. In order to compare the correlation effects, we plot the $A_{\rm hf}/g_I$ values from the DF method (given as O) and correlation contributions through the OT_1, OS_{1v} (after subtracting their respective lowest-order DF contributions) and OS_{2v} terms along with their Hermitian conjugate terms in Fig. 2. For convenience, we plot results of the S, P, $D_{3/2}$, and $D_{5/2}$ states separately as have been shown in the figure. As expected, the DF results are larger in all the cases except for the $D_{5/2}$ states, implying that only an all-order perturbative method is suitable for carrying out the calculations accurately in these states. In most of the states, core-valence effects are negligibly small except for the ground state where these effects contribute to some extent. Except for the $D_{5/2}$ states, pair-correlation effects through the OS_{1v} term seem to contribute significantly, but with opposite sign relative to the DF results. However, the next dominant contribution comes from the core-polarization effects through the OS_{2v} term and has the same sign as the DF values for these states. The final results arise from the strong cancellations between these contributions. On the other hand, core-polarization effects through the OS_{2v} term make the largest correlation contributions in the evaluation of $A_{\rm hf}/g_I$ as in the case of the alkaline-earth-metal ions [26] and have opposite sign relative to their DF values. In these states too, the core-valence and pair-correlation effects contribute with negative sign to their DF values except in the $6D_{3/2}$ state. Again, by comparing all the plots one can easily notice that the correlation effects in the lower-lying states for each angular momentum are large compared to their corresponding high-lying states.

Having described the correlation trends in the evaluation of the $A_{\rm hf}/g_I$ values in different states, we now proceed to comprehend these trends for the $B_{\rm hf}/Q$ results for the states with angular momenta $J > 1/2$. Plots for these results are shown in Fig. 3 for the $P_{3/2}$, $D_{3/2}$, and $D_{5/2}$ states separately. Clearly, the correlation trends for the $B_{\rm hf}/Q$ results

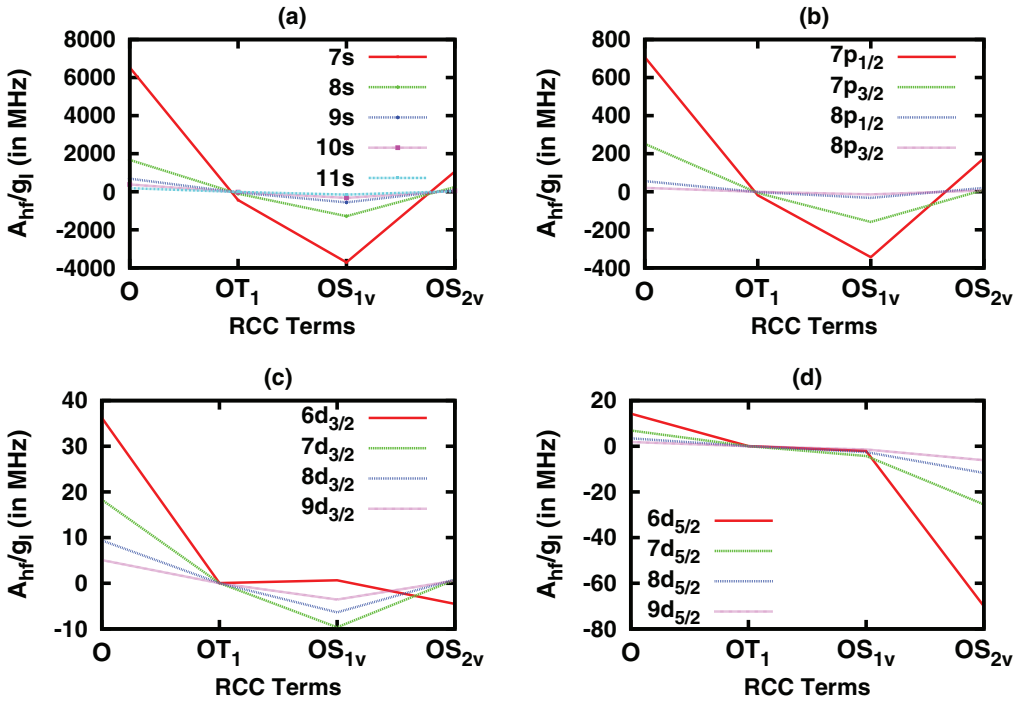

FIG. 2. (Color online) Demonstration of correlation trends in the evaluation of $A_{\rm hf}/g_I$ values (in MHz) in a Fr atom through a few important CCSD terms. Results among the considered (a) S, (b) P, (c) $D_{3/2}$, and (d) $D_{5/2}$ states are compared from the DF, OT_1, OS_{1v} (after subtracting the DF value), and OS_{2v} terms along with their Hermitian conjugate terms in a sequence in each arbitrary unit distance.

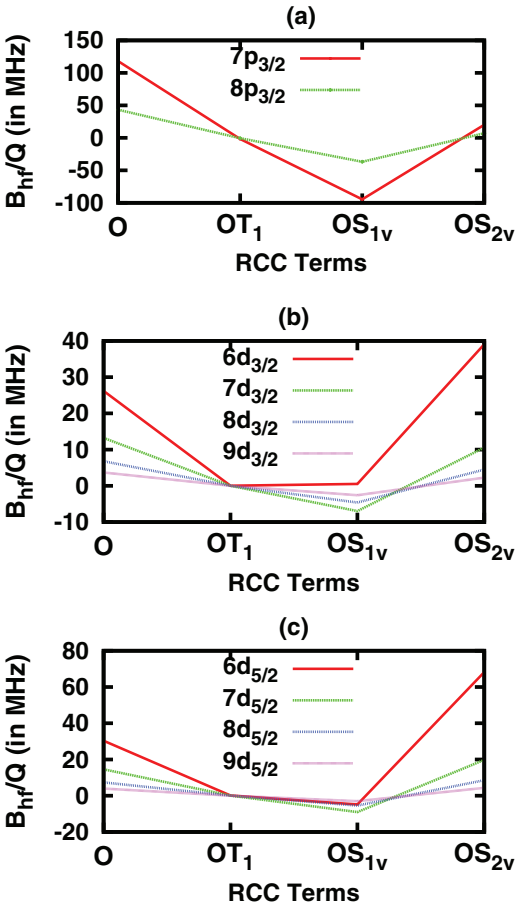

FIG. 3. (Color online) Comparison of correlation trends in the evaluation of $B_{\rm hf}/Q$ values (in MHz) of the considered states of Fr through a few important CCSD terms. Results among the considered (a) $P_{3/2}$, (b) $D_{3/2}$, and (c) $D_{5/2}$ states are compared from the DF, OT_1, OS_{1v} (after subtracting the DF value), and OS_{2v} terms along with their Hermitian conjugate terms in a sequence in each arbitrary unit distance.

are different from those of the $A_{\rm hf}/g_I$ values, although both the hyperfine interaction operators are of even parity and originate from the nucleus. The reason for these differences could be due to different angular momentum selection rules for their evaluations. In general, both the DF and core-polarization effects contribute to $B_{\rm hf}/Q$ results with positive sign and the DF values are larger in the $P_{3/2}$ states while core-polarization effects are larger in the D states. The core-valence and pair-correlation effect contributions have negative sign with smaller magnitudes.

We list the calculated and experimental values of $A_{\rm hf}$ and $B_{\rm hf}$ of ^{210}Fr and ^{212}Fr in Table III for which a few high-precision measurements are available. Coc *et al.* obtained the $A_{\rm hf}$ value for the ground $7S$ state as 7195.1(4) MHz using high-resolution spectroscopy [27]. In the same work, Coc *et al.* had also given $A_{\rm hf}$ and $B_{\rm hf}$ values of the $7P_{3/2}$ state as 78.0(2) MHz and 51(4) MHz, respectively. Using the two-photon excitation spectroscopy of a ^{210}Fr atom confined and cooled in a magneto-optical trap, Simsarian *et al.* obtained the experimental $A_{\rm hf}$ value for the $8S$ state as 1577.8(23) MHz at the ISOLDE facility [13]. Fairly recently, Gomez *et al.* measured the $A_{\rm hf}$ value for the $9S$ state as 622.25(36) MHz using a similar experimental technique [15]. From another experiment, Coc *et al.* reported the $A_{\rm hf}$ value of the $7P_{1/2}$ state as 945.6(5.8) MHz [28]. A more precise value of $A_{\rm hf}$ in the $7P_{1/2}$ state was obtained by Grossman *et al.* as 946.6(5.8) MHz [12]. Soon after that Grossman *et al.* extracted the $A_{\rm hf}$ values for the $7D_{3/2}$ and $7D_{5/2}$ states by measuring hyperfine splittings as 22.3(5) MHz and $-17.8(8)$ MHz, respectively [14]. Here, they had neglected the $B_{\rm hf}$ value of the $7D_{3/2}$ state while estimating a large $B_{\rm hf}$ value as 64(17) MHz for the $7D_{5/2}$ state. Similarly, for the ^{212}Fr isotope there are many experimental results available for the $A_{\rm hf}$ and $B_{\rm hf}$ values measured using various spectroscopic techniques, which are presented in the same Table III. For instance Coc *et al.*, adopting the same experimental technique as for ^{210}Fr, measured the $A_{\rm hf}$ values of the $7S$ and $7P_{1/2,3/2}$ states in ^{212}Fr [27,28]. It can be noticed from the tabulated results for the $A_{\rm hf}$ values that there is excellent agreement between the present calculations with the experimental values of the $7P_{1/2,3/2}$ states, where our results differ from the measurements by about 1.2% for the ground state. In another experiment Duong *et al.* used stepwise laser excitation in collinear geometry with the online mass separator of the ISOLDE facility at CERN and measured the $A_{\rm hf}$ and $B_{\rm hf}$ values for the $7S$, $7P$, and $8P$ states of ^{212}Fr [29]. Our calculations are also in good agreement with these experimental results for the above states. Arnold *et al.* further extended this project to carry out measurements of the hyperfine structure constants of the $10S$, $11S$, $8D$, and $9D$ states in ^{212}Fr [16], which are also given in Table III. It can be seen that these results and our calculations agree very well.

As has been stated before, the evaluation of the theoretical results for $A_{\rm hf}$ and $B_{\rm hf}$ require the knowledge of the g_I (i.e., μ_I and I) and Q values of the atom. Our calculations using our CCSD$_{\rm t3}$ method are the most rigorous theoretical results to date as they take into account more physical effects than the previous calculations. The current best value of μ_I in ^{210}Fr was extracted by combining the experimental $A_{\rm hf}$ value of its $9S$ state with the corresponding calculation using the SDpT method [15]. However, if experimental results for the hyperfine structure constants of any state are known to high precision, the extraction of nuclear moments from these measurements can be justified. In reality, most of the measured $A_{\rm hf}$ values in ^{210}Fr are known quite precisely among which the ground-state result is the most accurate (see Table III). To infer a g_I value for ^{210}Fr from the $A_{\rm hf}$ results, we take the mean value from the data obtained combining the measurements with their corresponding calculations using the CCSD$_{\rm t3}$ method for all the states except for the $D_{5/2}$ states. The reason for not considering the results of these states is that the correlation effects in these cases are more than 100% while for other states the principal contributions come from the DF values. In this approach, we obtain $g_I = 0.733765942$ which corresponds to $\mu_I = 4.40(5)$ of ^{210}Fr. Here only the uncertainties from the measurements are taken into account. This value is in agreement with its earlier reported values as $\mu_I = 4.40(9)$ [30] and $\mu_I = 4.38(5)$ [15], which were also determined by a similar approach. Unlike the case of $A_{\rm hf}$, only two experimental values for $B_{\rm hf}$ in ^{210}Fr have been reported,

TABLE III. Comparison between the theoretically determined and experimentally available A_{hf} and B_{hf} results for ^{210}Fr and ^{212}Fr with the uncertainties given in the parentheses. Theoretical results are obtained by combining the $CCSD_{t3}$ values from Table II with the deduced nuclear moments in this work.

	^{210}Fr				^{212}Fr			
	A_{hf} (MHz)		B_{hf} (MHz)		A_{hf} (MHz)		B_{hf} (MHz)	
States	$CCSD_{t3}$	Expt.	$CCSD_{t3}$	Expt.	$CCSD_{t3}$	Expt.	$CCSD_{t3}$	Expt.
$7s\ ^2S_{1/2}$	7254(75)	7195.1(4)[a]			9124(94)	9064.2(2)[a]		
						9064.4(1.5)[b]		
$7p\ ^2P_{1/2}$	939(7)	945.6(5.8)[c]			1181(9)	1189.1(4.6)[c]		
		946.3(2)[d]				1187.1(6.8)[b]		
						1192.0(2)[d]		
$7p\ ^2P_{3/2}$	77(2)	78.0(2)[a]	51.9(8)	51(4)[a]	96(3)	97.2(1)[a]	−26.0(4)	−26.0(2)[b]
						97.2(1)[b]		
$6d\ ^2D_{3/2}$	63(4)		19.3(6)		79(5)		−9.9(3)	
$6d\ ^2D_{5/2}$	−43(4)		25.8(8)		−54(5)		−13.1(4)	
$8s\ ^2S_{1/2}$	1579(15)	1577.8(23)[e]			1986(19)			
$8p\ ^2P_{1/2}$	295(4)				371(5)	373.0(1)[b]		
$8p\ ^2P_{3/2}$	26(2)		16.5(2)		32(3)	32.8(1)[b]	−8.4(1)	−7.7(9)[b]
$7d\ ^2D_{3/2}$	23(2)	22.3(5)[f]	6.0(4)	Assume 0[f]	29(3)		−3.1(2)	
$7d\ ^2D_{5/2}$	−12(2)	−17.8(8)[f]	7.8(2)	64(17)[f]	−15(3)		−4.0(1)	
$9s\ ^2S_{1/2}$	624(7)	622.25(36)[g]			784(9)			
$10s\ ^2S_{1/2}$	333(7)				419(9)	401(5)[h]		
$8d\ ^2D_{3/2}$	11(1)		2.7(2)		13(1)	13.0(6)[h]	−1.4(1)	Assume 0[h]
$8d\ ^2D_{5/2}$	−5(1)		3.5(1)		−6(1)	−7.1(6)[h]	−1.78(5)	−2(10)[h]
$9d\ ^2D_{3/2}$	6(1)		1.4(1)		7(1)	7.1(7)[h]	−0.72(5)	Assume 0[h]
$9d\ ^2D_{5/2}$	−2.6(5)		1.8(1)		−3.3(6)	−3.6(4)[h]	−0.94(5)	Assume 0[h]
$11s\ ^2S_{1/2}$	169(7)				212(9)	225(3)[h]		

[a]Reference [27].
[b]Reference [29].
[c]Reference [28].
[d]Reference [12].
[e]Reference [13].
[f]Reference [14].
[g]Reference [15].
[h]Reference [16].

among which the result for the $7D_{5/2}$ state might have been overestimated given that the wave function of the $7D_{5/2}$ state can have an extremely small overlap in the nuclear region. Note that B_{hf} of the $7P_{3/2}$ state is 51(4) MHz. Thus, combining the B_{hf} value of the $7P_{3/2}$ state with the corresponding calculation, we obtain $Q = 0.196(15)b$, where the uncertainty only from the measurement is taken into account, and the value estimated earlier was $Q = 0.19(2)b$ [30] for ^{210}Fr. The agreement between these two values is because the same experimental B_{hf} value has been used in both the results. By substituting these revised μ_I and Q values, we have evaluated the theoretical A_{hf} and B_{hf} values of ^{210}Fr and they are reported in Table III. We have also given the uncertainties of our calculated values by roughly estimating the contributions from the triple excitations that would modify the wave functions and also the possible error due to the truncation in the basis functions used for the construction of the atomic orbitals. This is not the actual uncertainty since the correlation effects coming through the full triple excitations could be much more significant in this heavy system which needs to be verified by considering more powerful CC methods.

Keeping in mind the small differences among the calculations of the values of A_{hf}/g_I and B_{hf}/Q between ^{210}Fr and ^{212}Fr, as was mentioned earlier, we expect to observe the ratios between the A_{hf} and B_{hf} values from ^{210}Fr and ^{212}Fr for any given state to be almost equal to ratios of their μ_I and Q values, respectively, as demonstrated in Ref. [31]. Considering all the experimental values known for the common states in both the isotopes, we find $g_I(^{212}\text{Fr})/g_I(^{210}\text{Fr}) = 1.25(1)$ and $Q(^{212}\text{Fr})/Q(^{210}\text{Fr}) = -0.51(5)$. Experimental results for A_{hf} and B_{hf} are reported for more states in ^{212}Fr than ^{210}Fr. Excluding A_{hf} results for the $D_{5/2}$ states owing to the reason stated previously, we obtain $g_I = 0.923070701$ for ^{212}Fr when we combine its experimental A_{hf} values of the remaining states with their respective A_{hf}/g_I calculations. This corresponds to $\mu_I(^{212}\text{Fr}) = 4.61(4)$. This, again, agrees with the previously reported value $\mu_I(^{212}\text{Fr}) = 4.62(9)$ [30]. In a similar procedure, we get $Q(^{212}\text{Fr}) = -0.10(1)b$ which is the same as that given in Ref. [30]. From these theoretical results, we get $g_I(^{212}\text{Fr})/g_I(^{210}\text{Fr}) = 1.26$ and $Q(^{212}\text{Fr})/Q(^{210}\text{Fr}) \approx -0.51$, which are in reasonable agreement with the estimated values from the measurements. Combining the respective nuclear moments, we have given the calculated values of the

hyperfine structure constants of ^{212}Fr in Table III along with their estimated uncertainties.

Comparison of the theoretical and experimental $A_{\rm hf}$ and $B_{\rm hf}$ results that are given in Table III are satisfactory for almost all the states, but we find a large discrepancy between the experimental and theoretical $B_{\rm hf}$ values for the $7D_{5/2}$ state. This result requires further theoretical and experimental verifications. Also, it was assumed that the $B_{\rm hf}$ values of other $D_{3/2,5/2}$ states were negligible while extracting the experimental $A_{\rm hf}$ values of the corresponding states; however, the present work shows that $B_{\rm hf}$ of the $7D_{3/2}$ state is about 6 MHz.

It is also worth mentioning that reasonable agreement between our calculations with the available experimental data of the hyperfine structure constants suggests that our calculated values of $A_{\rm hf}/g_I$ and $B_{\rm hf}/Q$ are quite accurate. Since calculations of these quantities do not depend much on the size of the isotopes in the absence of anomalies, our $A_{\rm hf}/g_I$ and $B_{\rm hf}/Q$ values can be used to estimate the $A_{\rm hf}$ and $B_{\rm hf}$ hyperfine structure constants in other isotopes of Fr by multiplying them with their respective nuclear moments (also possibly rescaling them with the knowledge of anomaly effects such as from Refs. [12,23,30]).

V. CONCLUSION

In summary, we have employed many-body methods at different levels of approximation to study the magnetic dipole and electric quadrupole hyperfine structure constants of the first 17 states in ^{210}Fr and ^{212}Fr. This work demonstrates the importance of the inclusion of the nonlinear terms in the coupled-cluster method to account for the contributions of important triples and quadrupole excitations for the accurate evaluation of the above-mentioned quantities that are necessary for the studies of the violations of parity and time reversal symmetries in Fr. By combining the experimental values with our corresponding calculations, we obtain $\mu_I = 4.40(5)$ and $Q = 0.196(15)b$ for ^{210}Fr and $\mu_I = 4.64(4)$ and $Q = 0.10(1)b$ for ^{212}Fr. Theoretical and experimental results are found to be in good agreement except for the electric quadrupole hyperfine structure constant of the $7D_{5/2}$ state. Theoretically predicted values for the hyperfine structure constants of many states including the $6D$ states, in the present work, could be tested experimentally in the future. Our calculations can also be used to estimate hyperfine structure constants of other isotopes of Fr with the knowledge of their respective nuclear moments.

ACKNOWLEDGMENTS

This work was supported partly by INSA-JSPS under Project No. IA/INSA-JSPS Project/2013-2016/February 28,2013/4098. Computations were carried out using the 3TFLOP HPC cluster at Physical Research Laboratory, Ahmedabad.

[1] Y. Sakemi, K. Harada, T. Hayamizu, M. Itoh, H. Kawamura, S. Liu, H. S. Nataraj, A. Oikawa, M. Saito, T. Sato, H. P. Yoshida, T. Aoki, A. Hatakeyama, T. Murakami, K. Imai, K. Hatanaka, T. Wakasa, Y. Shimizu, and M. Uchida, J. Phys.: Conf. Ser. **302**, 012051 (2011).

[2] G. Stancari, S. N. Atutov, R. Calabrese, L. Corradi, A. Dainelli, C. de Mauro, A. Khanbekyan, E. Mariotti, P. Minguzzi, L. Moi, S. Sanguinetti, L. Tomassetti, and S. Veronesi, Eur. Phys. J. Spec. Top. **150**, 389 (2007).

[3] T. Dreischuh, E. Taskova, E. Borisova, and A. Serafetinides, in *Proceedings of the 15th International School on Quantum Electronics: Laser Physics and Applications* (SPIE, Bellingham, WA, 2008), Vol. 7027, pp. 70270C-70270C-7.

[4] E. Gomez, S. Aubin, G. D. Sprouse, L. A. Orozco, and D. P. DeMille, Phys. Rev. A **75**, 033418 (2007).

[5] I. I. Sobelman, in *Atomic Spectra and Radiative Transitions* (Springer-Verlag, Berlin, 1979), p. 156.

[6] B. K. Sahoo, G. Gopakumar, R. K. Chaudhuri, B. P. Das, H. Merlitz, U. S. Mahapatra, and D. Mukherjee, Phys. Rev. A **68**, 040501(R) (2003).

[7] B. K. Sahoo, R. Pandey, and B. P. Das, Phys. Rev. A **84**, 030502(R) (2011).

[8] M. Vajed-Samii, J. Andriessen, B. P. Das, S. N. Ray, Taesul Lee, and T. P. Das, Phys. Rev. Lett. **49**, 1800 (1982).

[9] M. Vajed-Samii, J. Andriessen, B. P. Das, S. N. Ray, Taesul Lee, and T. P. Das, Phys. Rev. Lett. **49**, 1466 (1982).

[10] M. Vajed-Samii, J. Andriessen, B. P. Das, S. N. Ray, T. Lee, and T. P. Das, J. Phys. B: At. Mol. Phys. **15**, L379 (1982).

[11] A. Owusu, R. W. Dougherty, G. Gowri, T. P. Das, and J. Andriessen, Phys. Rev. A **56**, 305 (1997).

[12] J. S. Grossman, L. A. Orozco, M. R. Pearson, J. E. Simsarian, G. D. Sprouse, and W. Z. Zhao, Phys. Rev. Lett. **83**, 935 (1999).

[13] J. E. Simsarian, W. Z. Zhao, L. A. Orozco, and G. D. Sprouse, Phys. Rev. A **59**, 195 (1999).

[14] J. M. Grossman, R. P. Fliller, III, T. E. Mehlstäubler, L. A. Orozco, M. R. Pearson, G. D. Sprouse, and W. Z. Zhao, Phys. Rev. A **62**, 052507 (2000).

[15] E. Gomez, S. Aubin, L. A. Orozco, G. D. Sprouse, E. Iskrenova-Tchoukova, and M. S. Safronova, Phys. Rev. Lett. **100**, 172502 (2008).

[16] E. Arnold, W. Borchers, H. T. Duong, P. Juncar, J. Lerme, P. Lievens, W. Neu, R. Neugart, M. Pellarin, J. Pinard, J. L. Vialle, K. Wendt (ISOLDE Collaboration), J. Phys. B. At. Mol. Opt. Phys. **23**, 3511 (1990).

[17] C. Schwartz, Phys. Rev. **97**, 380 (1955).

[18] I. Lindgren and J. Morrison, *Atomic Many-Body Theory*, 2nd ed. (Springer-Verlag, Berlin, 1986).

[19] A. Szabo and N. Ostuland, *Modern Quantum Chemistry*, 1st ed. (Dover Publications, Mineola, NY, 1996).

[20] I. Shavitt and R. J. Bartlett, *Many-Body Methods in Chemistry and Physics* (Cambridge University Press, Cambridge, UK, 2009).

[21] I. Angeli, At. Data Nucl. Data Tables **87**, 185 (2004).

[22] M. S. Safronova, W. R. Johnson, and A. Derevianko, Phys. Rev. A **60**, 4476 (1999).

[23] V. A. Dzuba, V. V. Flambaum, and O. P. Sushkov, J. Phys. B: At. Mol. Phys. **17**, 1953 (1984).

[24] J.-L. Heully and A.-M. Mårtensson-Pendrill, Phys. Rev. A **27**, 3332 (1983).

[25] B. K. Sahoo, S. Majumder, R. K. Chaudhuri, B. P. Das, and D. Mukherjee, J. Phys. B **37**, 3409 (2004).

[26] B. K. Sahoo, C. Sur, T. Beier, B. P. Das, R. K. Chaudhuri, and D. Mukherjee, Phys. Rev. A **75**, 042504 (2007).

[27] A. Coc, C. Thibault, F. Touchard, H. T. Duong, P. Juncar, S. Liberman, J. Pinard, J. Lerme, J. L. Vialle, S. Büttgenbach, A. C. Mueller, A. Pesnelle (ISOLDE Collaboration), Phys. Lett. B **163**, 66 (1985).

[28] A. Coc, C. Thibault, F. Touchard, H. T. Duong, P. Juncar, S. Liberman, J. Pinard, M. Carre, J. Lerme, J. L. Vialle, S. Büttgenbach, A. C. Mueller, A. Pesnelle (ISOLDE Collaboration), Nucl. Phys. A **468**, 1 (1987).

[29] H. T. Duong, P. Juncar, S. Liberman, A. C. Mueller, R. Neugart, E. W. Otten, B. Peuse, J. Pinard, H. H. Stroke, C. Thibault, F. Touchard, J.-L. Vialle, K. Wendt (ISOLDE Collaboration), Europhys. Lett. **3**, 175 (1987).

[30] C. Ekström, L. Robertsson, and A. Rosen, Phys. Scr. **34**, 624 (1986).

[31] B. K. Sahoo, M. D. Barrett, and B. P. Das, Phys. Rev. A **87**, 042506 (2013).